

## THE MULTI-KINASE INHIBITOR EC-70124 SYNERGISTICALLY INCREASED THE ANTI-TUMOR ACTIVITY OF DOXORUBICIN IN SARCOMAS

**Running Title:** Synergistic combination of EC-70124 and doxorubicin in sarcoma.

Oscar Estupiñan<sup>1,2,3</sup>, Laura Santos<sup>1</sup>, Aida Rodriguez<sup>1</sup>, Lucía Fernandez-Nevaldo<sup>1</sup>, Paula Costales<sup>4</sup>, Jhudit Perez-Escuredo<sup>4</sup>, Maria Ana Hermosilla<sup>4</sup>, Patricia Oro<sup>4</sup>, Veronica Rey<sup>1,2</sup>, Juan Tornín<sup>1,2</sup>, Eva Allonca<sup>1</sup>, Maria Teresa Fernández-García<sup>5</sup>, Carlos Alvarez-Fernández<sup>6</sup>, Alejandro Braña<sup>7</sup>, Aurora Astudillo<sup>8</sup>, Sofia T Menendez<sup>1,2,3</sup> Francisco Morís<sup>4</sup> and Rene Rodriguez<sup>1,2,3</sup>\*

<sup>1</sup>Hospital Universitario Central de Asturias - Instituto de Investigación Sanitaria del Principado de Asturias, Oviedo, Spain; <sup>2</sup>Instituto Universitario de Oncología del Principado de Asturias, Oviedo, Spain. <sup>3</sup>CIBER en oncología (CIBERONC), Madrid, Spain. <sup>4</sup>EntreChem SL, Oviedo, Spain.

<sup>5</sup>Unidad Histopatología Molecular en Modelos Animales de Cáncer, IUOPA, Universidad de Oviedo, Oviedo, Spain. <sup>6</sup>Servicio de Oncología Médica, <sup>7</sup>Servicio de Traumatología and <sup>8</sup>Servicio de Anatomía Patológica of the Hospital Universitario Central de Asturias, Oviedo, Spain.

### (\*) Correspondence should be addressed to:

Rene Rodriguez, PhD

Laboratorio ORL–IUOPA, Hospital Universitario Central de Asturias - Instituto de Investigación Sanitaria del Principado de Asturias. Av. de Roma s/n, 33011 Oviedo, SPAIN.

Phone: 00 34 985107956

Email: renerg.finba@gmail.com, rodriguezrene.uo@uniovi.es

**Keywords:** EC-70124, indolocarbazole, sarcoma, myxoid liposarcoma, doxorubicin, mTOR, ABC pumps, drug resistance

**Conflict of interest disclosure statement:** P.C., J.P-E., M-A.H, P.O and F.M are employees of EntreChem SL. F.M reports ownership of stock in EntreChem SL. All other authors declare they have no competing interests. This does not alter adherence to International Journal of Cancer policies on sharing data and materials.

**Word count:** 4750

**Number of figures and/or tables:** 6 figures

### Abbreviations:

MSC: mesenchymal stromal/stem cells

BMSC: bone marrow-derived mesenchymal stem/stromal cell

ABC: ATP binding cassette

PI3K: phosphatidylinositol-3' kinase

mTOR: mammalian target of rapamycin

MRCLS: myxoid/round cell liposarcoma  
FUS: fused in sarcoma  
CHOP: C/EBP homologous protein  
S6: ribosomal protein S6  
4EBP1: eukaryotic initiation factor 4E-binding protein-1  
RTK: receptor tyrosine kinase  
IGF1R: insulin-like growth factor I receptor  
PDGFR: platelet-derived growth factor receptor  
FGFR: fibroblast growth factor receptor  
AML: acute myeloid leukemia  
H&E: hematoxylin and eosin  
FFPE: Formalin-fixed paraffin-embedded  
FNCLCC: French Federation of Comprehensive Cancer Centers  
CI: combination index  
CSC: cancer stem cell

**Article category:** Research article - Cancer Therapy and Prevention

**Novelty and Impact:** Anti-tumor therapies directed against aberrantly activated kinases frequently trigger the activation of compensatory routes that cause adaptive resistance. In an effort to overcome this effect we evaluated the activity of the indolocarbazole EC-70124 in sarcoma. This compound acts as a wide spectrum multi-kinase inhibitor and show strong anti-proliferative effects. Importantly, EC-70124 inhibits several ABC pumps resulting in increased anti-tumor activity of doxorubicin, thus providing a rationale for the testing of this combination in sarcoma patients.

## ABSTRACT

Cytotoxic drugs like doxorubicin remain as the most utilized agents in sarcoma treatment. However, advanced sarcomas are often resistant, thus stressing the need for new therapies aimed to overcome this resistance. Multi-kinase inhibitors provide an efficient way to target several pro-tumorigenic pathways using a single agent and may constitute a valuable strategy in the treatment of sarcomas, which frequently show an aberrant activation of pro-tumoral kinases. Therefore, we studied the antitumor activity of EC-70124, an indolocarbazole analog that have demonstrated a robust ability to inhibit a wide range of pro-survival kinases. Evaluation of the phospho-kinase profile in cell-of-origin sarcoma models and/or sarcoma primary cell lines evidenced that PI3K/AKT/mTOR, JAK/STAT or SRC were among the most highly activated pathways. In striking contrast with the structurally related drug midostaurin, EC-70124 efficiently prevented the phosphorylation of these targets and robustly inhibited proliferation through a mechanism associated to the induction of DNA damage, cell cycle arrest and apoptosis. In addition, EC-70124 was able to partially reduce tumor growth *in vivo*. Importantly, this compound inhibited the expression and activity of ABC efflux pumps involved in drug resistance. In line with this ability, we found that the combined treatment of EC-70124 with doxorubicin resulted in a synergistic cytotoxic effect *in vitro* and an increased anti-tumor activity of this cytotoxic drug *in vivo*. Altogether, these results uncover the capability of the novel multikinase inhibitor EC-70124 to counteract drug resistance in sarcoma and highlight its therapeutic potential when combined with current treatments.

## INTRODUCTION

Sarcomas comprise a group of aggressive malignancies which are suggested to develop from transformed mesenchymal stromal/stem cells (MSCs).<sup>1,2</sup> Despite advances in the clinical management of these diseases the overall survival for patients presenting with metastatic and recurrent disease continues to be dismal<sup>3</sup> and cytotoxic drugs like doxorubicin remain as the mainstay for first-line treatments.<sup>4,5</sup> However, advanced sarcomas often show resistance to doxorubicin, mainly through the overexpression of members of ATP binding cassette (ABC) transmembrane family of transporters which act as efflux pumps for anti-cancer drugs.<sup>6</sup> Therefore, the development of therapeutic strategies able to prevent drug resistance would undoubtedly improve current sarcoma treatments.<sup>7,8</sup>

The phosphatidylinositol-3' kinase (PI3K)/AKT/mammalian target of rapamycin (mTOR) signaling pathway is abnormally activated in many sarcomas and alterations in several components of this axis have been correlated with poor clinical outcome.<sup>9-12</sup> Specifically, myxoid and round cell liposarcomas (MRCLS), an adipocytic tumor characterized by the expression of the fusion oncogene FUS-CHOP, frequently show oncogenic events, such as mutations in *PI3KCA* or overactivation of insulin-like growth factor I receptor (IGF1R) or SRC signaling, which provoke an abnormal activation of these route.<sup>13-18</sup>

mTOR is a serine/threonine protein kinase that exists in two different complexes (mTORC1 and mTORC2). Activated mTORC1 phosphorylates its downstream targets S6 kinase-1, which in turn phosphorylates/activates the ribosomal protein S6 (S6), and the eukaryotic initiation factor 4E-binding protein-1 (4EBP1) resulting in the activation of the synthesis of a panoply of proteins involved in cell growth, metabolism and survival.<sup>11,19</sup> On the other hand, the activation of mTORC2 is involved in actin remodeling and may also contribute to complete activation of mTORC1 through the activation of AKT earlier in the pathway.<sup>9,19</sup> Upstream, the PI3K/AKT/mTOR

pathway may be triggered by the activation several receptor tyrosine kinases (RTKs), such as IGF1R, platelet-derived growth factor receptor (PDGFR) or fibroblast growth factor receptor (FGFR), and non-receptor tyrosine kinases, like SRC, whose deregulation reportedly plays a role in the tumorigenic process in several types of sarcoma.<sup>15,17,18,20</sup>

Consistent with these findings, the efficiency of several mTOR inhibitors have been evaluated in sarcomas.<sup>9</sup> Clinical testing of rapamycin and its derived analogs has provided at best only modest results.<sup>21</sup> This limited response may be explained by the fact that these compounds are efficient inhibitors of mTORC1 but not mTORC2 which contribute to induce an adaptive resistance due to the reactivation of AKT.<sup>22</sup> Therefore, a new generation of inhibitors able to target both complexes and/or combinatorial strategies aimed to prevent resistance to mTOR inhibitors are being tested in sarcomas.<sup>22-24</sup>

Targeting several key oncogenic signals with a single agent may constitute an ideal alternative to increase efficiency and prevent the activation of resistance mechanisms. In line with this aim, EC-70124 is a hybrid indolocarbazole analog<sup>25</sup> with a potent multikinase inhibitor spectrum affecting key signaling kinases implicated in pro-survival and proliferative pathways. Thus, EC-70124 have shown antitumor activity in breast, glioblastoma, colorectal and prostate tumors as well as in acute myeloid leukemia (AML) associated to the inhibition of a wide variety of targets including components of the PI3K/AKT/mTOR, JAK/STAT, NFκB or FLT3 pathways.<sup>26-30</sup> Interestingly, midostaurin (PKC-412), an indolocarbazole clinically approved for AML treatment, has shown anti-tumor activity in certain sarcoma subtypes.<sup>31-33</sup>

Here, we evaluated the anti-tumor effect properties of EC-70124 and midostaurin in relevant sarcoma models and patient-derived primary cell lines. Opposite to midostaurin, EC-70124 showed strong anti-proliferative effects through a mechanism mediated by mTOR inhibition. In addition, this drug inhibited the expression and activity of ABC transporters and synergized in vitro and in vivo with doxorubicin, thus highlighting the therapeutic potential of this combination.

## MATERIALS AND METHODS

### Cell culture, drugs and ethics statement.

Transformed bone marrow-derived mesenchymal stem/stromal cell (hBMSC) lines with or without expression of FUS-CHOP were previously generated and characterized (Table S1 and Supplemental Information;<sup>34,35</sup>). Patient-derived primary cell cultures were generated as described in Supplemental Information. An overview of patient and tumor characteristics is given in table S2. The identity of all cell lines has been authenticated by Short Tandem Repeats analysis during the last 3 months. All the cell lines were tested for Mycoplasma monthly using the LONZA MycoAlert Mycoplasma Detection Kit (LONZA, Rockland CE) and cultured as previously described.<sup>34</sup> EC-70124 was synthesized by a proprietary process by EntreChem S.L. (Oviedo, Spain). PKC-412 (midostaurin) was synthesized from staurosporine (Biomar Microbial Technologies, León, Spain) and the identity of the isolated product verified by comparison to an authentic sample (HPLC, NMR). Stocks of EC-70124, midostaurin, doxorubicin (Sigma, St Louis, MO), torin, sorafenib, pazopanib, imatinib, BYL-719, BP-1-102 and ruxolitinib (Selleckchem, Houston, TX) were prepared as 10 mM solutions in sterile DMSO for *in vitro* experiments, maintained at -20 °C, and brought to the final concentration just before use. For *in vivo* experiments, doxorubicin was prepared in sterile saline solution and administered intravenously and EC-70124 was dosed by oral gavage. Human samples and data from donors included in this study were provided by the Principado de Asturias BioBank (PT17/0015/0023) integrated in the Spanish National Biobanks Network. All experimental protocols have been performed in accordance with institutional review board guidelines and were approved by the Institutional Ethics Committee of the Hospital Universitario Central de Asturias.

### Tumorsphere culture

Tumorsphere formation protocol and the analysis of the effects of drugs on tumorsphere cultures were previously described.<sup>36</sup>

### **Cell viability assays**

The viability of all cell lines in the presence and absence of drugs was determined using the Cell Proliferation reagent WST-1 (Roche, Mannheim, Germany) as described before.<sup>37</sup> The concentration of half-maximal inhibition of viability ( $IC_{50}$ ) for each treatment was determined by non-linear regression using the graphPad Prism software (La Jolla, CA). The existence of synergy in drug combinations was determined by calculating the combination index (CI) as described in Supplemental information.

### **Western blotting and phospho-kinase antibody arrays**

Whole cell protein extraction and Western blotting analysis were performed as previously described.<sup>37</sup> Antibodies used are described in Supplemental Information.

The phosphorylation status of a wide range of RTKs and downstream signaling nodes was evaluated in EC-70124 or midostaurin-treated cells using the PathScan RTK Signaling Antibody Array Kit (# 7982, Cell Signaling Technology, Danvers, MA). Protein extraction after treatments, array incubation and signal development was performed using the reagents provided by the kit according to the manufacturer's instructions.

Infrared fluorescent signals in Western blotting and antibody array analysis were detected and quantified using a Odyssey Fc imaging system and the software Image Studio from LICOR (Lincoln, NE). The signal intensity of the background was subtracted from the signal of each spot, and the average of duplicate spots was determined. Next, normalized signal intensity was calculated by dividing the mean value in each spot over the mean value in the positive control.

### **Cell-cycle analysis**

Cell-cycle analysis was carried out as described previously.<sup>4</sup>

### **Immunofluorescence staining**

In  $\gamma$ H2AX immunofluorescence experiments, fixation, staining and mounting of the samples were performed as previously reported.<sup>4</sup> Antibodies and experimental conditions are described in Supplemental Information.

### **RT-qPCR assays**

The expression of ABCB1 and ABCG2 was assessed by qPCR as described in Supplemental Information.

### **Transporter substrate and inhibition assays**

The assessment of the ability of EC-70124 to inhibit ACBB1/MDR1 and ABCG2/BCRP1 or to be a substrate for these transporters were performed by Absorption Systems (Exton, PA) as described in Supplemental Information.

### ***In vivo* tumor growth**

All experimental protocols were carried out in accordance with the institutional guidelines of the University of Oviedo and were approved by the Animal Research Ethical Committee of the University of Oviedo prior to the study. Female NOD/SCID mice of 6 weeks old (Janvier Labs, St Berthevin, France) were inoculated subcutaneously (s.c.) with  $2 \times 10^6$  T5H-FC#1 cells. Once tumors reached 200-300 mm<sup>3</sup>, the mice were randomly assigned to receive vehicle, EC-70124 (80 mg/Kg, q2dx11, orally), doxorubicin (4 mg/Kg, q4dx3, intra-venous) or the combination of EC-70124 (40 mg/Kg, q2dx8, orally) and doxorubicin (4 mg/Kg, q4dx3, intravenous), intra-venous. Animals were sacrificed by CO<sub>2</sub> asphyxiation when tumors of the control series reached approximately 1000 mm<sup>3</sup> or if severe weight loss were observed. Mean tumor volume differences between groups were determined using a caliper (Supplemental Information). The student *t* test



was performed to determine the statistical significance between different groups. The F-test was used to compare tumor volume growth kinetics. Drug efficacy was expressed as the percentage tumor growth inhibition (%TGI) (Supplemental Information). For pharmacodynamic studies, a single dose of each treatment was inoculated into immunodeficient mice carrying tumors of approximately 400-500 mm<sup>3</sup>. Tumors (n=2/3 per group) were collected after 4, 24 or 48 hours, minced, washed with PBS and homogenized in ice-cold lysis buffer (1mL/100 mg of tumor; see Supplemental Information for buffer composition) using a GentleMACS Dissociator system (Miltenyi Biotec, Bergisch Gladbach, Germany) according to manufacturer instructions. This homogenate was centrifuged at 10,000 xg for 20 minutes at 4°C, and the supernatants containing protein extracts were transferred to new tubes and used in Western blotting experiments.

#### **Histological analysis.**

Tumor samples were fixed in formol, embedded in paraffin, cut into 4-µm sections, and stained with hematoxylin and eosin (H&E). Tumor sections were also subjected to immunohistochemistry as previously reported<sup>38</sup> using the antibodies and quantification methods described in Supplemental Information. Tumor grade was analyzed in H&E stained preparations using the French Federation of Comprehensive Cancer Centers (FNCLCC) grading system (Supplemental Information).

## RESULTS

### Differential effects of the indolocarbazole analogs EC-70124 and midostaurin in sarcoma.

To study the anti-tumor effects of indolocarbazole analogs in sarcoma we used previously developed cell-of-origin models of undifferentiated pleomorphic sarcoma (MSC-4H-GFP, MSC-5H-GFP and T-5H-GFP#1) and FUS-CHOP (FC)-expressing MRCLS (MSC-4H-FC, MSC-5H-FC, T-4H-FC#3 and T-5H-FC#1) in which hBMSCs were sequentially mutated with up to six oncogenic events (see Table S1 and Supplemental information). The evaluation of cell toxicity in dose-response experiments showed that, opposite to wild type hBMSCs, all sarcoma models were sensitive to nanomolar concentrations of EC-70124 ( $IC_{50}$  values between 180 and 540 nM) (Figure 1A-B). To further characterize the cytotoxic effect of EC-70124 we performed similar dose-response experiments in a panel of primary sarcoma cell lines (described in Table S2 and Supplemental information). A subgroup of 5 primary cell lines (CDS1, CDS17, SARC6 and CDS11) show a sensitivity to EC-70124 similar to that observed for the sarcoma models ( $IC_{50}$  values between 201 and 343 nM), while another 3 cell lines (SARC1, SARC3 and SARC4) were more resistant ( $IC_{50}$  values between 705 nM and 1.3  $\mu$ M) (Figure 1C). In accordance with this cytotoxic effect, EC-70124 treatment induced a dose-dependent apoptotic cleavage of PARP both in sarcoma models (MSC-5H-FC and T-5H-FC#1 cells) (Figure 1D) and primary cell lines (Figure 1E). In striking contrast to the effect of EC-70124, sarcoma models MSC-5H-FC and T-5H-FC#1 were resistant to the treatment with the structurally related compound midostaurin (Figure S1A-B) and this drug induced only a marginal apoptotic effect compared to that of EC-70124 (Figure 1D). As a control, midostaurin was efficient inhibiting proliferation of a leukemia cell line as previously shown<sup>29</sup> (Figure S1A). Cell cycle analysis also showed a different response of sarcoma cells to the treatment with both indolocarbazole analogs. Cell cycle profiles of MSC-5H-FC and T-5H-FC#1 cells treated with 1  $\mu$ M EC-70124 were characterized by a strong arrest in S-

phase followed by the induction of high levels of apoptosis (Sub-G<sub>1</sub> population). On the other hand, cells treated with 1  $\mu$ M midostaurin quickly arrest in G<sub>2</sub>/M phase and underwent endoreplication without cell division resulting in cell populations with 8n DNA content after 48 hours of treatment (Figure 1F). In line with the different ability to induce S-phase arrest, EC-70124, but not midostaurin, was able to efficiently induce DNA damage in T-5H-FC cells as indicated by the dose-dependent increase of intranuclear  $\gamma$ H2AX foci levels (Figure 1G-H and Figure S2).

Next, we tested the ability of these indolocarbazole analogs to target cancer stem cell (CSC)-enriched tumorsphere cultures of MSC-5H-FC and T-5H-FC#1 cells.<sup>36</sup> Again, EC-70124 was more efficient than midostaurin in eliminating CSCs (Figure S1C), although its cytotoxic effect on CSC subpopulations was lower than that previously observed in non-selected adherent cultures (Figure 1A-B) and also much lower than the effect of the mythramycin analog EC-8042, a drug with reported activity on sarcoma CSCs.<sup>37</sup>

Finally, to compare the cytotoxic effect of EC-70124 with other multikinase inhibitors already approved for cancer treatment, we treated T-5H-FC#1 cells with increasing concentrations of sorafenib, pazopanib and imatinib. All of these drugs were much more inefficient than EC-70124 in reducing cell survival, showing IC<sub>50</sub> concentrations of 20  $\mu$ M or higher (Figure S3).

### **Effect of EC-70124 and midostaurin on the kinase profile of sarcomas**

To gain insights about the mechanistic basis of EC-70124-induced cytotoxicity in sarcomas, we used phospho-kinase antibody arrays to evaluate the ability of the indolocarbazole analogs to inhibit the phosphorylation/activation of 39 relevant receptor tyrosine kinases and signaling transducers. In T-5H-FC#1 cells, EC-70124 induced an efficient and durable inhibition of several components of the PI3K/AKT/mTOR and MAPK pathways, including phospho-AKT (T308 and

S473), phospho-S6 (S235/236) and phospho-ERK1/2 (T202/Y204) (Figure 2A-B, Figure S4A and Figure S5). On the other hand, midostaurin produced a much reduced and reversible inhibition of these targets (Figure 2A-B). Western blotting analyses of time-course (Figure 2C) and dose-response experiments (Figure 2D) confirmed that EC-70124 is much more efficient than midostaurin in inhibiting the phosphorylation of AKT and the mTOR downstream targets S6 and 4EBP1 in MRCLS models, without affecting total protein levels. Complementary, we calculated the inhibitor binding constants ( $K_d$  values) for a panel of kinases in the presence of several concentrations of EC-70124 or midostaurin (KdELECT assay, DiscoverX). Similar to that observed measuring phosphorylation levels, EC-70124 showed a higher potency than midostaurin to bind/inhibit mTOR signaling (S6K1, RSK2, RSK3 and RSK4) and cell cycle-related kinases (CHK1, AURKA, AURKB and AURKC) (Table S3).

As in T5H-FC#1 cells, AKT, S6 and ERK1/2 were the kinases/signaling molecules showing a higher level of activation/phosphorylation in three sarcoma primary cell lines. Again, EC-70124 was able to inhibit the phosphorylation of these targets, with the only exception of ERK1/2 in the line CDS1+ and AKT (S473) in the line SARC6+ (Figure 2E-F, Figure S4C and Figure S5). Of note, the inhibition of phospho-S6 was complete in all the assayed cell lines. In addition, some of the primary cell lines also displayed high levels of phospho-STAT1 (CDS17+ and SARC6+), phospho-STAT3 (CDS1+, CDS17+ and SARC6+) and phospho-SRC (CDS1+ and SARC6+) and EC-70124 efficiently inhibited these phosphorylations (Figure 2E-F). In Western blotting analysis of dose-response experiments we confirmed the ability of EC-70124 to inhibit the phosphorylation of phospho-AKT, phospho-S6 and phospho-STAT3 in six primary cell lines (Figure 2G).

Overall these results indicate that EC-70124 is a more efficient multi-kinase inhibitor and show a more robust anti-proliferative effect than midostaurin in sarcomas. Also, they suggest that mTOR signaling inhibition may play a prominent role in EC-70124-induced cytotoxicity.

**mTOR signaling inhibition mediates EC-70124-induced cytotoxicity.**

To study the relevance of the contribution of mTOR signaling inhibition to the anti-tumor effects of EC-70124, we analyzed the effects of the well-known mTOR inhibitor torin in T-5H-FC#1 cells. As expected, torin was able to efficiently inhibit the phosphorylation of AKT, S6 and 4EBP1 (Figure S6A). We found that, compared to EC-70124 and midostaurin, torin showed an intermediate capacity to reduce cell viability (Figure S6B), and did not induce DNA damage (Figure S2). Given that torin is a potent mTOR inhibitor, we hypothesized that if the inhibition of mTOR signaling is involved in the mediation of the cytotoxic effect of EC-70124 we do not expect a great synergy from the combination of this indolocarbazole with torin. Conversely, given that midostaurin is a poor inhibitor of mTOR signaling, if the inhibition of mTOR signaling is a relevant mechanism we would expect a higher synergistic effect when we combine torin with midostaurin. Investigating this hypothesis we found that combination of EC-70124 or midostaurin with increasing concentrations of torin enhanced cytotoxicity (Figure S6C-D). However, by representing the data of these combinations normalized to the effect of torin alone, we did not find a relevant shift of toxicity curves in the combinations with EC-70124 (Figure S6E). Otherwise, we did find an important shift toward higher toxicity in the combinations of torin with midostaurin (Figure S6F), thus suggesting a more than additive contribution of the mTOR inhibitor to the toxicity of midostaurin. To test whether these combinations has synergistic cytotoxic effect we calculated their combination index (CI) using the CompuSyn software. In the case of combinations with EC-70124 we found an intermediate level of synergism (CI value for  $ED_{75}=0.44$ ) when we assay combinations of drugs that target between 40 and 75% of the cells ( $0.4 < Fa < 0.7$ ). However, this synergistic effect is lost at combinations of higher concentrations of drugs that affect a higher percentage of the cells ( $Fa > 0.8$ ) (Figure S6G). This effect may be explained by the fact that at high concentrations of EC-70124 mTOR signaling is completely inhibited and a mTOR signaling inhibitor like torin cannot add a further effect. On the other hand, and in line with our rationale, the

combination of increasing concentrations of torin with midostaurin resulted in a constant increase of the CI, which reached the level of strong synergism when the fraction of cells affected is higher than 70% (CI value for  $ED_{75}=0.14$ ) (Figure S6G).

To investigate whether the inhibition of other kinases may also play a role in EC-70124 anti-tumor effect, we tested the effect of a PI3K inhibitor (BYL-719), a STAT3 inhibitor (BP-1-102) and a JAK1/2 inhibitor (ruxolitinib) alone or in combinations on T-5H-FC#1 cells. Although at higher concentrations than EC-70124 or torin, BYL-719 was able to inhibit AKT and S6 phosphorylation. In addition, BP-1-102 and ruxolitinib inhibited STAT3 phosphorylation (Figure S7A). None of these inhibitors were efficient cytotoxic drugs, showing  $IC_{50}$  concentrations of 20  $\mu$ M or higher (Figure S7B-D). Moreover, the combination of BP-1-102 with BYL-719 did not produce any increase in cytotoxicity (Figure S7E).

Altogether, the combination of indolocarbazole analogs with torin suggested that the inhibition of the mTOR signaling plays a relevant role in anti-proliferative activity of EC-70124.

#### ***In vivo* anti-tumor activity of EC-70124.**

Oral treatment of NOD/SCID mice carrying T-5H-FC#1 xenografts with EC-70124 resulted in a moderate tumor growth inhibition. Compared to vehicle treated group, mice treated with 80 mg/Kg of EC-70124 every two days showed a percentage of TGI of 26.5% (Figure 3A). Likewise, at the end of the experiment, tumor weights of EC-70124-treated mice were significantly lower than those of the control group (Figure 3B). Notably, EC-70124 treatment did not cause loss of weight (Figure 3C) or other adverse effects. Histological examination of tumors showed that EC-70124-treated tumors exhibited lower mitotic counts and a significant reduction in tumor grade in comparison to untreated tumor samples (Figure 3D-E).

The pharmacodynamic profile of EC-70124 was obtained by analyzing protein levels in tumors collected at different time-points in a sub-cohort of mice (n=2-3) upon a single 80 mg/kg dose (Figure 3F). Pharmacodynamic effect of EC-70124 was in agreement with the results obtained in cultured cells. Thus, a partial inhibition of the phosphorylation of S6 and AKT was detected in tumor tissues 4 hours after the treatment, thus suggesting that same pathways identified *in vitro* are mediating the effects *in vivo* (Figure 3F). Recovery profile of the proteins analyzed showed that the inhibition of the phosphorylation of the mTOR target S6 was sustained for at least 24-48 hours after dosing, while phospho-AKT showed a faster recovery (Figure 3F).

**EC-70124 inhibits the expression and activity of ABC transporters and is not a substrate for them.**

Several ABC transporters, such as ABCG2/BCRP1 and ABCB1/MDR1, play major roles in drug resistance in tumor cells.<sup>6-8</sup> It has been previously reported that a panel of indolocarbazole protein kinase inhibitors, including midostaurin, were able to inhibit the transport activity of ABCG2.<sup>39,40</sup> Therefore we studied the interaction of EC-70124 with the two members of the ABC family most commonly involved in drug resistance of cancer cells. In functional assays we found that EC-70124 efficiently inhibited the pumping activity of both ABCG2 and ABCB1 (Figure 4A, Table S4 and Table S5) and moreover, these pumps failed to transport this indolocarbazole analog (Figure 4B and Table S6). Importantly, EC-70124 was also able to decrease the mRNA (Figure 4C) and protein (Figure 4D) expression of ABCG2 and ABCB1 in several MSC-5H and T-5H cell lines.

This inhibitory effect of EC-70124 on the expression and activity of ABC transporters suggest that, besides its anti-tumor activity, this drug may also play a role in counteracting drug resistance.

**EC-70124 and doxorubicin shows synergistic cytotoxic effect *in vitro* and *in vivo*.**

Doxorubicin-based therapies are still widely used as first-line treatments of both soft tissue and bone sarcomas.<sup>5</sup> However, doxorubicin, like many other chemotherapeutic agents, is a well-known substrate of ABC transporters.<sup>41</sup> Therefore, given the ability of EC-70124 to inhibit ABC transporters, we tested whether its combination with doxorubicin may produce a synergistic anti-tumor effect. First, we found that all sarcoma models were also sensitive to nanomolar concentrations of doxorubicin ( $IC_{50}$  values between 74 and 318 nM) (Figure S8). Doxorubicin treatment resulted in an up-regulation of phospho-S6, phospho-4EBP and ABCB1, while EC-70124, alone or in combination with doxorubicin efficiently decreased the levels of these targets (Figure 5A). Importantly, the combination of EC-70124 with 100 nM doxorubicin significantly shifted toxicity curves and markedly decreased the  $IC_{50}$  of EC-70124 in several sarcoma model cell lines but not in wild-type hMSCs (Figure 5B). By calculating the CI of several constant ration combinations of EC-70124 and doxorubicin, we confirmed the existence of synergism between both drugs in MSC-5H-FC (CI value for  $ED_{75}=0.30$ ) and T-5H-FC#1 cells (CI value for  $ED_{75}=0.62$ ) (Figure 5C).

*In vivo* activity of the combination was evaluated in T-5H-FC#1 xenografts treated with oral doses of 40mg/kg EC-70124 every two days and/or intra-venous doses of 4 mg/kg doxorubicin every four days. By measuring the evolution of tumor volumes during the treatment (Figure 6A) and tumor weights at the end of the experiments (Figure 6B), we found that, as previously showed, EC-70124 caused certain level of tumor growth inhibition (% TGI= 27.2), whereas doxorubicin was more efficient in inhibiting tumor growth (% TGI = 68.7). Importantly, the combination of EC-70124 and doxorubicin was able to reduce tumor volumes (% TGI= 93.7) in a nearly statistically significant fashion ( $P=0.09$ ) and tumor weights in a significant manner ( $P=0.01$ ) compared to the effect of both drugs alone (Figure 6A-B). Of note, mice treated with regimens including



doxorubicin experienced important weight loss and the experiment had to be suspended on day 14 (Figure 6C).

Pharmacodynamic analysis showed that EC-70124 was able to inhibit the phosphorylation of S6 and AKT even in the presence of doxorubicin, which increased the phosphorylation of S6 in individual treatments (Figure 6D). In addition, a notably increase in apoptosis (PARP cleavage) was detected in tumors treated with the combination (Figure 6D). Histological examination confirmed the inhibition of phospho-S6, in tumors treated with EC-70124 alone or in combination with doxorubicin (Figure 6E-F). In addition, tumors treated with doxorubicin alone or in combination with EC-70124 exhibited significantly reduced mitotic counts and tumor grade (Figure 6E-F).

Altogether, these results indicate that the combination of EC-70124 and doxorubicin has a synergistic anti-tumor effect on sarcoma.

## DISCUSSION

Indolocarbazole alkaloids have attracted great attention because of their original structural features and their ability to inhibit a wide spectrum of receptor and intracellular signaling kinases.<sup>25,42</sup> Among these compounds midostaurin have been recently approved for the treatment of AML patients harboring mutations in FLT3.<sup>43</sup> In sarcoma, this drug has been found to inhibit the transcriptional activity of fusion oncogenes characteristic of alveolar rhabdomyosarcoma (PAX3/FKHR) and Ewing sarcoma (EWS/FLI1) as well as exhibited anti-tumor potential in these and other types of sarcoma.<sup>31-33</sup> In addition, midostaurin has been show to synergize with anti-tumor agents like HDAC inhibitors, oncostatin M, or IGF1R inhibitors in different types of sarcoma.<sup>44,45</sup>

Here we found that the indolocarbazole analog EC-70124 is much more efficient that midostaurin in inhibiting the phosphorylation of ERK1/2 at Thr202 and Tyr204, AKT at Ser473 and Thr308, pS6 at Ser235 and Ser236 and 4EBP at Ser65, which are the kinases/kinase substrates more activated among a panel of relevant signaling molecules in a cell-of-origin model of MRCLS. In a similar way, EC-70124 has recently demonstrated a higher capacity than midostaurin to inhibit several clinically relevant kinases in pre-clinical models of AML.<sup>29</sup> In addition, EC-70124 was also able to inhibit the activation of SRC, STAT1 and STAT3 which were found activated in several primary sarcoma cell lines. This higher potential of EC-70124 as multi-kinase inhibitor in sarcomas correlated with a more potent anti-proliferative effect in comparison with midostaurin and the basis of this enhanced toxicity relies on the induction of much higher levels of DNA damage followed by a more stringent S-phase arrest and apoptosis. It has been reported that midostaurin and other indolocarbazoles inhibit Aurora kinase, resulting in abrogation of the mitotic spindle checkpoint and the accumulation of cells with 4N and 8N DNA content.<sup>46,47</sup> Here we

observed a similar effect after the treatment of sarcoma cells with midostaurin, although this endoreplication effect is not sufficient to efficiently reduce cell viability. *In vitro* kinase binding affinity assays showed that EC-70124 inhibited Aurora kinases even more potently than midostaurin (Table S3) and opposite to this drug, EC-70124 was also a powerful inhibitor of CHK1, which is a key player in the sensing and the response to DNA damage in the S and G<sub>2</sub> phases of cell cycle.<sup>48</sup> This differential ability of both drugs to inhibit CHK1 may be responsible for the pronounced S-phase arrest and the increased DNA damage and apoptosis observed after the treatment with EC-70124 but not with midostaurin.

Downstream mTORC1 effectors S6 and 4EBP were the targets whose phosphorylation levels were more consistently inhibited by EC-70124 in all the sarcomas cell lines tested. The efficient inhibition of the phosphorylation of S6 correlates with the high affinity (low K<sub>d</sub>) of EC-70124 for S6K1 (Table S3). This data are in line with previously reported activity of EC-70124 in breast and colon cancer.<sup>27,30</sup> By combining EC-70124 or midostaurin with the mTOR inhibitor torin, we studied the role of mTOR signaling in the cytotoxic effect of indolocarbazole analogs. Torin induced certain level of toxicity and did not synergize with EC-70124, which was an efficient mTOR inhibitor by itself and therefore did not allow for a mechanistic synergy with torin. On the other hand, torin synergized with midostaurin, which was a poor and transient inhibitor of mTOR signaling. Altogether, these results suggest that, although the inhibition of other targets could contribute, the blocking of mTOR signaling plays a key role in EC-70124-induced anti-proliferative effects.

Despite the relevant role that PI3K/AKT/mTOR pathway plays in the pathogenesis of several types of sarcomas, including MRCLS,<sup>14-16</sup> and the promising anti-tumor activity observed *in vitro*, EC-70124 showed only a small, although significant, effect *in vivo*. This effect was accompanied with a partial and durable inhibition of phospho-S6 and a transient inhibition of phospho-AKT (S473) which recovered pre-treatment levels after 24 hours. Several mechanisms of resistance

involving the recovering of PI3K/AKT signaling after the activation of mTORC2 via IGFR1 or PDGFR signaling have been described for different mTOR inhibitors.<sup>20,22,23</sup> Therefore, the restoring of AKT signaling may be in the basis of the resistance to the treatment with EC-70124. Nevertheless, we have not detected an increased phosphorylation of IGF1R or PDGFR after EC-70124-treatment *in vitro* (Figure S4), thus suggesting that other unknown mechanisms may be mediating the reactivation of AKT.

Signaling mediated by PI3K-AKT-mTOR has been involved in drug resistance in a wide range of tumors<sup>9,19</sup> Accordingly, mTOR inhibitors were able to restore sensitivity against tyrosin kinase inhibitors and chemotherapeutic drugs like doxorubicin, cisplatin or paclitaxel in several types of tumors including sarcomas.<sup>9,19,49</sup> Apart from the anti-apoptotic and pro-survival signals mediated by PI3K-AKT-mTOR signaling, the upregulation of members of ABC family of transporters through the activation of this pathway seems to be another important mechanism of drug resistance.<sup>19,50</sup> In these regard, several Indolocarbazoles have demonstrated its ability to inhibit ABCB1 and/or ABCG2 and reverse drug resistance.<sup>39,40</sup> In addition, several tyrosine kinase inhibitors have been recently reported to increase the efficacy of conventional chemotherapeutic agents through mechanisms involving the inhibition and/or the expression of different ABC pumps.<sup>8</sup> Here we found that EC-70124 was able to inhibit the enzymatic activity and the expression of ABCB1 and ABCG2 and moreover, it was not transported by these pumps. In line with this result, we showed that the combination of EC-70124 with doxorubicin produced a synergistic decrease of cell viability and a reduction in tumor growth *in vivo*. These findings suggest that the ability of EC-70124 to inhibit ABC transporters maybe in the basis of these enhanced anti-tumor potential of the combination.

Altogether, these results uncover the capability of the novel multikinase inhibitor EC-70124 to counteract drug resistance in sarcoma and provide a rationale for the clinical testing of the EC-70124 plus doxorubicin combination in sarcoma patients.

## ACKNOWLEDGEMENTS

This work was supported by the Agencia Estatal de Investigación (AEI) [MINECO/Fondo Europeo de Desarrollo Regional (FEDER) (RTC2016-4603-1 to EntreChem SL and SAF-2016-75286-R to R.R.), ISC III/FEDER [Miguel Servet Program (CPII16/00049 to R.R.), Sara Borrell Program (CD16/00103 to S-T.M.) and Consorcio CIBERONC (CB16/12/00390)] and the Plan de Ciencia Tecnología e Innovación del Principado de Asturias (GRUPIN14-003). We want to particularly acknowledge for its collaboration, the Principado de Asturias BioBank (PT17/0015/0023), financed jointly by Servicio de Salud del Principado de Asturias, Instituto de Salud Carlos III and Fundación Bancaria Cajastur and integrated in the Spanish National Biobanks Network.

## AUTHORSHIP CONTRIBUTIONS

**O.E., L.S., A.R, L.-FN. P.C., J.P-E., V.R., & J.T.:** development of methodology, performance of experimental procedures, acquisition, analysis and interpretation of data. **M-A.H., P.O. & E.A.:** performance of experimental procedures. **M-T.F-G., C.A-F., A.B., A.A. & S-T.M:** analysis and interpretation of data. **F.M.:** provision of key materials, analysis and interpretation of data and manuscript revision. **R.R:** Conception and design, analysis and interpretation of data, manuscript writing and financial support. The manuscript has been seen and approved by **all authors**.

**REFERENCES**

1. Abarrategi A, Tornin J, Martinez-Cruzado L, Hamilton A, Martinez-Campos E, Rodrigo JP, Gonzalez MV, Baldini N, Garcia-Castro J, Rodriguez R. Osteosarcoma: Cells-of-Origin, Cancer Stem Cells, and Targeted Therapies. *Stem Cells Int* 2016; 2016:3631764.
2. Rodriguez R, Rubio R, Menendez P. Modeling sarcomagenesis using multipotent mesenchymal stem cells. *Cell Res* 2012; 22:62-77.
3. Chen C, Borker R, Ewing J, Tseng WY, Hackshaw MD, Saravanan S, Dhanda R, Nadler E. Epidemiology, treatment patterns, and outcomes of metastatic soft tissue sarcoma in a community-based oncology network. *Sarcoma* 2014; 2014:145764.
4. Martinez-Cruzado L, Tornin J, Rodriguez A, Santos L, Allonca E, Fernandez-Garcia MT, Astudillo A, Garcia-Pedrero JM, Rodriguez R. Trabectedin and Camptothecin Synergistically Eliminate Cancer Stem Cells in Cell-of-Origin Sarcoma Models. *Neoplasia* 2017; 19:460-470.
5. Ratan R, Patel SR. Chemotherapy for soft tissue sarcoma. *Cancer* 2016; 122:2952-2960.
6. Szakacs G, Paterson JK, Ludwig JA, Booth-Genthe C, Gottesman MM. Targeting multidrug resistance in cancer. *Nat Rev Drug Discov* 2006; 5:219-234.
7. Bugde P, Biswas R, Merien F, Lu J, Liu DX, Chen M, Zhou S, Li Y. The therapeutic potential of targeting ABC transporters to combat multi-drug resistance. *Expert Opin Ther Targets* 2017; 21:511-530.
8. Wu S, Fu L. Tyrosine kinase inhibitors enhanced the efficacy of conventional chemotherapeutic agent in multidrug resistant cancer cells. *Mol Cancer* 2018; 17:25.
9. Blay JY. Updating progress in sarcoma therapy with mTOR inhibitors. *Ann Oncol* 2011; 22:280-287.
10. Dobashi Y, Suzuki S, Sato E, Hamada Y, Yanagawa T, Ooi A. EGFR-dependent and independent activation of Akt/mTOR cascade in bone and soft tissue tumors. *Mod Pathol* 2009; 22:1328-1340.
11. Saxton RA, Sabatini DM. mTOR Signaling in Growth, Metabolism, and Disease. *Cell* 2017; 168:960-976.
12. Setsu N, Kohashi K, Fushimi F, Endo M, Yamamoto H, Takahashi Y, Yamada Y, Ishii T, Yokoyama K, Iwamoto Y, Oda Y. Prognostic impact of the activation status of the Akt/mTOR pathway in synovial sarcoma. *Cancer* 2013; 119:3504-3513.
13. Barretina J, Taylor BS, Banerji S, Ramos AH, Lagos-Quintana M, Decarolis PL, Shah K, Succi ND, Weir BA, Ho A, Chiang DY, Reva B, Mermel CH, Getz G, Antipin Y, Beroukhim R, Major JE, Hatton C, Nicoletti R, Hanna M, Sharpe T, Fennell TJ, Cibulskis K, Onofrio RC, Saito T, Shukla N, Lau C, Nelander S, Silver SJ, Sougnez C, Viale A, Winckler W, Maki RG, Garraway LA, Lash A, Greulich H, Root DE, Sellers WR, Schwartz GK, Antonescu CR, Lander ES, Varmus HE, Ladanyi M, Sander C, Meyerson M, Singer S. Subtype-specific genomic alterations define new targets for soft-tissue sarcoma therapy. *Nat Genet* 2010; 42:715-721.

14. Demicco EG, Torres KE, Ghadimi MP, Colombo C, Bolshakov S, Hoffman A, Peng T, Bovee JV, Wang WL, Lev D, Lazar AJ. Involvement of the PI3K/Akt pathway in myxoid/round cell liposarcoma. *Mod Pathol* 2012; 25:212-221.
15. Patel RB, Li T, Liao Z, Jaldeepbhai JA, Perera H, Muthukuda SK, Dhirubhai DH, Singh V, Du X, Yang J. Recent translational research into targeted therapy for liposarcoma. *Stem Cell Investig* 2017; 4:21.
16. Sanfilippo R, Dei Tos AP, Casali PG. Myxoid liposarcoma and the mammalian target of rapamycin pathway. *Curr Opin Oncol* 2013; 25:379-383.
17. Tornin J, Hermida-Prado F, Padda RS, Gonzalez MV, Alvarez-Fernandez C, Rey V, Martinez-Cruzado L, Estupinan O, Menendez ST, Fernandez-Nevado L, Astudillo A, Rodrigo JP, Lucien F, Kim Y, Leong HS, Garcia-Pedrero JM, Rodriguez R. FUS-CHOP Promotes Invasion in Myxoid Liposarcoma through a SRC/FAK/RHO/ROCK-Dependent Pathway. *Neoplasia* 2018; 20:44-56.
18. Trautmann M, Menzel J, Bertling C, Cyra M, Isfort I, Steinestel K, Elges S, Grunewald I, Altvater B, Rossig C, Frohling S, Hafner S, Simmet T, Aman P, Wardelmann E, Huss S, Hartmann W. FUS-DDIT3 Fusion Protein-Driven IGF-1R Signaling is a Therapeutic Target in Myxoid Liposarcoma. *Clin Cancer Res* 2017; 23:6227-6238.
19. Jiang BH, Liu LZ. Role of mTOR in anticancer drug resistance: perspectives for improved drug treatment. *Drug Resist Updat* 2008; 11:63-76.
20. Ho AL, Vasudeva SD, Lae M, Saito T, Barbashina V, Antonescu CR, Ladanyi M, Schwartz GK. PDGF receptor alpha is an alternative mediator of rapamycin-induced Akt activation: implications for combination targeted therapy of synovial sarcoma. *Cancer Res* 2012; 72:4515-4525.
21. Mita MM, Gong J, Chawla SP. Ridaforolimus in advanced or metastatic soft tissue and bone sarcomas. *Expert Rev Clin Pharmacol* 2013; 6:465-482.
22. Lamhamedi-Cherradi SE, Menegaz BA, Ramamoorthy V, Vishwamitra D, Wang Y, Maywald RL, Buford AS, Fokt I, Skora S, Wang J, Naing A, Lazar AJ, Rohren EM, Daw NC, Subbiah V, Benjamin RS, Ratan R, Priebe W, Mikos AG, Amin HM, Ludwig JA. IGF-1R and mTOR Blockade: Novel Resistance Mechanisms and Synergistic Drug Combinations for Ewing Sarcoma. *J Natl Cancer Inst* 2016; 108.
23. May CD, Landers SM, Bolshakov S, Ma X, Ingram DR, Kivlin CM, Watson KL, Sanna GAA, Bhalla AD, Wang WL, Lazar AJ, Torres KE. Co-targeting PI3K, mTOR, and IGF1R with small molecule inhibitors for treating undifferentiated pleomorphic sarcoma. *Cancer Biol Ther* 2017; 18:816-826.
24. Slotkin EK, Patwardhan PP, Vasudeva SD, de Stanchina E, Tap WD, Schwartz GK. MLN0128, an ATP-competitive mTOR kinase inhibitor with potent in vitro and in vivo antitumor activity, as potential therapy for bone and soft-tissue sarcoma. *Mol Cancer Ther* 2015; 14:395-406.
25. Sanchez C, Salas AP, Brana AF, Palomino M, Pineda-Lucena A, Carbajo RJ, Mendez C, Moris F, Salas JA. Generation of potent and selective kinase inhibitors by combinatorial biosynthesis of glycosylated indolocarbazoles. *Chem Commun (Camb)* 2009:4118-4120.
26. Civenni G, Longoni N, Costales P, Dallavalle C, Garcia Inclan C, Albino D, Nunez LE, Moris F, Carbone GM, Catapano CV. EC-70124, a Novel Glycosylated Indolocarbazole Multikinase Inhibitor, Reverts Tumorigenic and Stem Cell Properties in Prostate Cancer by Inhibiting STAT3 and NF-kappaB. *Mol Cancer Ther* 2016; 15:806-818.

27. Cuenca-Lopez MD, Serrano-Heras G, Montero JC, Corrales-Sanchez V, Gomez-Juarez M, Gascon-Escribano MJ, Morales JC, Voisin V, Nunez LE, Moris F, Bader GD, Pandiella A, Ocana A. Antitumor activity of the novel multi-kinase inhibitor EC-70124 in triple negative breast cancer. *Oncotarget* 2015; 6:27923-27937.
28. Nogueira L, Ruiz-Ontanon P, Vazquez-Barquero A, Lafarga M, Berciano MT, Aldaz B, Grande L, Casafont I, Segura V, Robles EF, Suarez D, Garcia LF, Martinez-Climent JA, Fernandez-Luna JL. Blockade of the NFkappaB pathway drives differentiating glioblastoma-initiating cells into senescence both in vitro and in vivo. *Oncogene* 2011; 30:3537-3548.
29. Puente-Moncada N, Costales P, Antolin I, Nunez LE, Oro P, Hermosilla MA, Perez-Escuredo J, Rios-Lombardia N, Sanchez-Sanchez AM, Luno E, Rodriguez C, Martin V, Moris F. Inhibition of FIt3 and Pim Kinases by Ec-70124 Exerts Potent Activity in Preclinical Models of Acute Myeloid Leukemia. *Mol Cancer Ther* 2018.
30. Serrano-Heras G, Cuenca-Lopez MD, Montero JC, Corrales-Sanchez V, Morales JC, Nunez LE, Moris F, Pandiella A, Ocana A. Phospho-kinase profile of colorectal tumors guides in the selection of multi-kinase inhibitors. *Oncotarget* 2015; 6:31272-31283.
31. Amstutz R, Wachtel M, Troxler H, Kleinert P, Ebauer M, Haneke T, Oehler-Janne C, Fabbro D, Niggli FK, Schafer BW. Phosphorylation regulates transcriptional activity of PAX3/FKHR and reveals novel therapeutic possibilities. *Cancer Res* 2008; 68:3767-3776.
32. Boro A, Pretre K, Rechfeld F, Thalhammer V, Oesch S, Wachtel M, Schafer BW, Niggli FK. Small-molecule screen identifies modulators of EWS/FLI1 target gene expression and cell survival in Ewing's sarcoma. *Int J Cancer* 2012; 131:2153-2164.
33. Kawamoto T, Akisue T, Kishimoto K, Hara H, Imabori M, Fujimoto T, Kurosaka M, Hitora T, Kawaguchi Y, Yamamoto T. Inhibition of PKCalpha activation in human bone and soft tissue sarcoma cells by the selective PKC inhibitor PKC412. *Anticancer Res* 2008; 28:825-832.
34. Rodriguez R, Rosu-Myles M, Arauzo-Bravo M, Horrillo A, Pan Q, Gonzalez-Rey E, Delgado M, Menendez P. Human bone marrow stromal cells lose immunosuppressive and anti-inflammatory properties upon oncogenic transformation. *Stem Cell Reports* 2014; 3:606-619.
35. Rodriguez R, Tornin J, Suarez C, Astudillo A, Rubio R, Yauk C, Williams A, Rosu-Myles M, Funes JM, Boshoff C, Menendez P. Expression of FUS-CHOP fusion protein in immortalized/transformed human mesenchymal stem cells drives mixoid liposarcoma formation. *Stem Cells* 2013; 31:2061-2072.
36. Martinez-Cruzado L, Tornin J, Santos L, Rodriguez A, Garcia-Castro J, Moris F, Rodriguez R. Aldh1 Expression and Activity Increase During Tumor Evolution in Sarcoma Cancer Stem Cell Populations. *Sci Rep* 2016; 6:27878.
37. Tornin J, Martinez-Cruzado L, Santos L, Rodriguez A, Nunez LE, Oro P, Hermosilla MA, Allonca E, Fernandez-Garcia MT, Astudillo A, Suarez C, Moris F, Rodriguez R. Inhibition of SP1 by the mithramycin analog EC-8042 efficiently targets tumor initiating cells in sarcoma. *Oncotarget* 2016; 7:30935-30950.
38. Rubio R, Abarrategi A, Garcia-Castro J, Martinez-Cruzado L, Suarez C, Tornin J, Santos L, Astudillo A, Colmenero I, Mulero F, Rosu-Myles M, Menendez P, Rodriguez R. Bone environment is essential for osteosarcoma development from transformed mesenchymal stem cells. *Stem Cells* 2014; 32:1136-1148.



39. Robey RW, Shukla S, Steadman K, Obrzut T, Finley EM, Ambudkar SV, Bates SE. Inhibition of ABCG2-mediated transport by protein kinase inhibitors with a bisindolylmaleimide or indolocarbazole structure. *Mol Cancer Ther* 2007; 6:1877-1885.
40. Utz I, Hofer S, Regenass U, Hilbe W, Thaler J, Grunicke H, Hofmann J. The protein kinase C inhibitor CGP 41251, a staurosporine derivative with antitumor activity, reverses multidrug resistance. *Int J Cancer* 1994; 57:104-110.
41. Wu D, Liu L, Yan X, Wang C, Wang Y, Han K, Lin S, Gan Z, Min D. Pleiotrophin promotes chemoresistance to doxorubicin in osteosarcoma by upregulating P-glycoprotein. *Oncotarget* 2017; 8:63857-63870.
42. Gallogly MM, Lazarus HM. Midostaurin: an emerging treatment for acute myeloid leukemia patients. *J Blood Med* 2016; 7:73-83.
43. Manley PW, Weisberg E, Sattler M, Griffin JD. Midostaurin, a Natural Product-Derived Kinase Inhibitor Recently Approved for the Treatment of Hematological Malignancies Published as part of the Biochemistry series "Biochemistry to Bedside". *Biochemistry* 2018; 57:477-478.
44. Brounais B, Chipoy C, Mori K, Charrier C, Battaglia S, Pilet P, Richards CD, Heymann D, Redini F, Blanchard F. Oncostatin M induces bone loss and sensitizes rat osteosarcoma to the antitumor effect of Midostaurin in vivo. *Clin Cancer Res* 2008; 14:5400-5409.
45. Radic-Sarikas B, Tsafou KP, Emdal KB, Papamarkou T, Huber KV, Mutz C, Toretsky JA, Bennett KL, Olsen JV, Brunak S, Kovar H, Superti-Furga G. Combinatorial Drug Screening Identifies Ewing Sarcoma-specific Sensitivities. *Mol Cancer Ther* 2017; 16:88-101.
46. Kawai M, Nakashima A, Kamada S, Kikkawa U. Midostaurin preferentially attenuates proliferation of triple-negative breast cancer cell lines through inhibition of Aurora kinase family. *J Biomed Sci* 2015; 22:48.
47. Stolz A, Vogel C, Schneider V, Ertych N, Kienitz A, Yu H, Bastians H. Pharmacologic abrogation of the mitotic spindle checkpoint by an indolocarbazole discovered by cellular screening efficiently kills cancer cells. *Cancer Res* 2009; 69:3874-3883.
48. Rodriguez R, Gagou ME, Meuth M. Apoptosis induced by replication inhibitors in Chk1-depleted cells is dependent upon the helicase cofactor Cdc45. *Cell Death Differ* 2008; 15:889-898.
49. Squillace RM, Miller D, Cookson M, Wardwell SD, Moran L, Clapham D, Wang F, Clackson T, Rivera VM. Antitumor activity of ridaforolimus and potential cell-cycle determinants of sensitivity in sarcoma and endometrial cancer models. *Mol Cancer Ther* 2011; 10:1959-1968.
50. Lee JT, Jr., Steelman LS, McCubrey JA. Phosphatidylinositol 3'-kinase activation leads to multidrug resistance protein-1 expression and subsequent chemoresistance in advanced prostate cancer cells. *Cancer Res* 2004; 64:8397-8404.

## LEGENDS TO FIGURES

**Figure 1. Antiproliferative effects of EC-70124 and midostaurin in sarcoma.** (A-C) Cell viability (WST1 assay) measured after the treatment of wild-type hMSCs and the indicated MSC-4H, T-4H (A), MSC-5H and T-5H cells lines (B) or several patient-derived sarcoma primary lines (C) with increasing concentrations of EC-70124 for 48 hours. IC<sub>50</sub> values for each cell type are shown. Error bars represent the standard deviation of at least three independent experiments. (D-E) Apoptotic cleavage of PARP in MSC-5H-FC and T-5H-FC#1 cells (D) or several primary cell lines (E) treated with the indicated concentrations of EC-70124 or midostaurin for 24 hours. The expression of  $\beta$ -actin was used as loading control in Western blotting analysis. (F) Time-course evolution of the cell cycle distribution of MSC-5H-GFP and MSC-5H-FC cells treated with 1 $\mu$ M EC-70124 or midostaurin. Peaks of cell populations with 2n, 4n and 8n DNA content, as well as the SubG1 population, are indicated. (G-H) Analysis of  $\gamma$ H2AX foci formation after the treatment of T-5H-FC#1 cells for 6 hours with the indicated concentrations of EC-70124 or midostaurin. (G) Quantification of  $\gamma$ H2AX foci was performed by counting more than 200 cells in each condition. The percentage of cells presenting high (>10 foci) or low level (<10 foci) of DNA damage is displayed. Error bars represent the standard deviation. (H) Representative merged images ( $\gamma$ H2AX immunodetection and DAPI staining) of immunostaining experiments showing a dose-dependent increase in  $\gamma$ H2AX foci formation following EC-70124 treatment. Scale bars= 50  $\mu$ m. A version of this panel showing separate  $\gamma$ H2AX-associated and DAPI fluorescence is displayed as Figure S2.

**Figure 2. Kinase inhibitory profile of EC-70124 and midostaurin.** (A & E) Phospho-kinase antibody arrays showing the phosphorylation/activation status of a panel of kinases in T-5H-FC#1

cells after the indicated treatments with EC-70124 or midostaurin (A) or in four primary sarcoma cell lines treated or not with 1  $\mu$ M EC-70124 for 24 hours (E). (B & F) Quantification of the levels of the indicated phospho-proteins in the kinase arrays loaded with T-5H-FC#1 (B) or sarcoma primary cell lines samples (F). Complete images of the phospho-kinase antibody arrays and the quantification of all analyzed kinases in T-5H-FC#1 and primary cell lines are presented as Figures S3A&C and S4 respectively. (C, D & G) Western blotting analysis of the indicated indicated proteins in T-5H-FC#1 cells treated with 1 $\mu$ M EC-70124 or midostaurin for the indicated times (C), in MSC-5H-FC and T-5H-FC#1 cells treated with the indicated concentrations of EC-70124 for 24 hours (D) and in a panel of primary cell lines treated for 24 hours with the indicated concentrations of EC-70124 (G). Error bars in protein quantifications represent the standard deviation of two duplicates.

**Figure 3. *In vivo* anti-tumor activity of EC-70124.** NOD/SCID mice with established T-5H-FC#1 tumor xenografts were randomly assigned to three different groups (n=7 *per* group) and treated by oral gavage with either vehicle or EC-70124 at 80 mg/kg every two days. (A) Curves representing the mean tumor volume of T-5H-FC#1 xenografts during the treatments. Drug efficacy expressed as the percentage of TGI at day 21 is indicated. (B) Tumor weight at the end of the experiment. (C) Body weights of mice during the treatments. (D-E) Pathological analysis of formalin-fixed paraffin embedded xenografts extracted from mice treated as in panel A. (D) Representative images of the H&E staining of control and EC-70124-treated tumors. Mitotic cells (red arrows) are indicated. Scale bars= 50  $\mu$ m. (E) Quantification of mitosis [number of mitotic figures per 10 high power fields (40X)] and tumor grade score according to FNCLCC system in tumors from the indicated series. (F) intra-tumor phosphorylation levels (Western blotting analysis) of the key targets (G) in samples collected at the indicated time-points from mice treated with a single oral dose of 80 mg/kg EC-70124. Error bars represent the SEM and asterisks

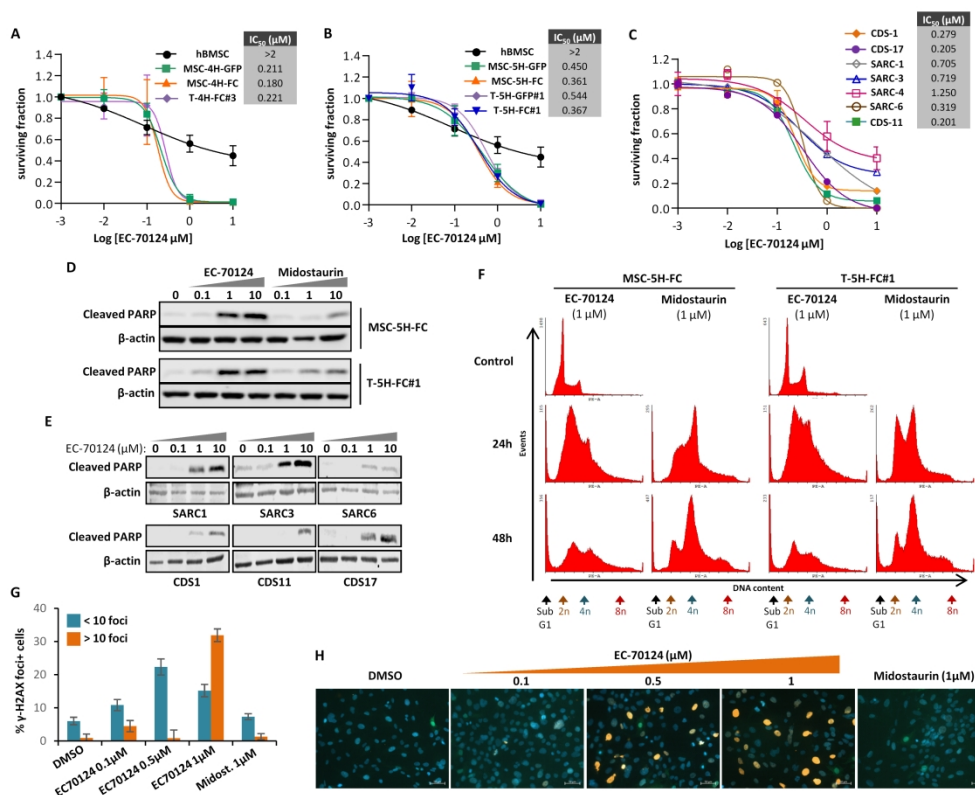
indicate statistically significant differences between EC-70124-treated and control groups (\*:p<0.05; two-sided Student *t* test).

**Figure 4. Effect of EC-70124 on ABC transporters expression and activity.** (A) ABCG2 and ABCB1 functional inhibition assay for EC-70124. Cladribine and digoxin were used as known substrates and Ko243 and valsopodar were used as known inhibitors for ABCG2 and ABCB1 respectively. A complete summary of experimental results is shown in Tables S3 and S4. (B) ABCG2 and ABCB1 functional substrate assay for EC-70124. Ko243 and valsopodar were used as transporter inhibitors for ABCG2 and ABCB1 respectively. A complete summary of experimental results is shown in Table S5. (C) Relative mRNA expression of ABCG2 and ABCB1 genes in MSC-5H-GFP and MSC-5H-FC cells treated with the indicated concentrations of EC-70124 for 24 hours. Error bars represents the standard deviation of three independent experiments and asterisks indicate a statistically significant difference with the respective untreated samples (\*:p<0.05; two-sided Student *t* test). (D) Western blotting analysis of ABCG2, ABCB1 and  $\beta$ -actin after the indicated treatments with EC-70124.

**Figure 5. EC-70124 and doxorubicin shows synergistic cytotoxic effect.** (A) Western blotting analysis of the indicated proteins after the indicated treatments with EC-70124 and/or doxorubicin. (B) Cell viability curves representing the IC<sub>50</sub> shift observed after 48 hours-treatments of the indicated cell lines with EC70124 alone or in combination with 0.1  $\mu$ M doxorubicin. Error bars represents the standard deviation of three independent experiments. (C) Combination index plots (mean and standard deviation) for constant ratio combinations of EC-70124 and doxorubicin (1:1) in MSC-5H-FC and T-5H-FC cells generated using the CompuSyn software. The CI ( $\pm$  standard deviation) values for ED<sub>50</sub>, ED<sub>75</sub> and ED<sub>90</sub> combination doses as calculated by the median effect equation are shown.

**Figure 6. *In vivo* effect of EC-70124 and doxorubicin combination.** T-5H-FC#1 established xenografts were randomly assigned to four different groups ( $n=7$  per group) and treated with vehicle(s), with EC-70124 (orally) at a dose of 40 mg/kg every two days, with doxorubicin (intravenous) at a dose of 4 mg/kg on days 0, 4 and 8, or with a combination of both drugs. (A) Curves representing the mean tumor volume of T-5H-FC#1 xenografts during the treatments. Drug efficacy expressed as the percentage of TGI at day 14 is indicated. (B) Tumor weight at the end of the experiment. (C) Body weights of mice during the treatments. (D) Intra-tumor phosphorylation levels (Western blotting analysis) of the key targets in samples collected following 0 and 4 hours of a single dose of the previously described treatments. (E-F) Pathological analysis of formalin-fixed paraffin embedded xenografts extracted from mice treated as in panel A. (E) H&E staining and immuno-staining detection of phospho-S6. mitotic cells (red arrows) are indicated. Scale bars= 50  $\mu\text{m}$ . (F) Quantification of tumor-related features including mitosis [number of mitotic figures per 10 high power fields (40X)] and tumor grade score according to FNCLCC system and levels of phospho-S6 [number of cell showing positive staining per 10 high power fields (40X)] in tumors from the indicated series. Error bars represent the SEM and asterisks indicate statistically significant differences between groups. Extra sum-of-squares F Test were used in panel A and Two-sided Student  $t$  test were used in panels B,D and G (\*: $p<0.05$ ; \*\*: $p<0.01$ );).

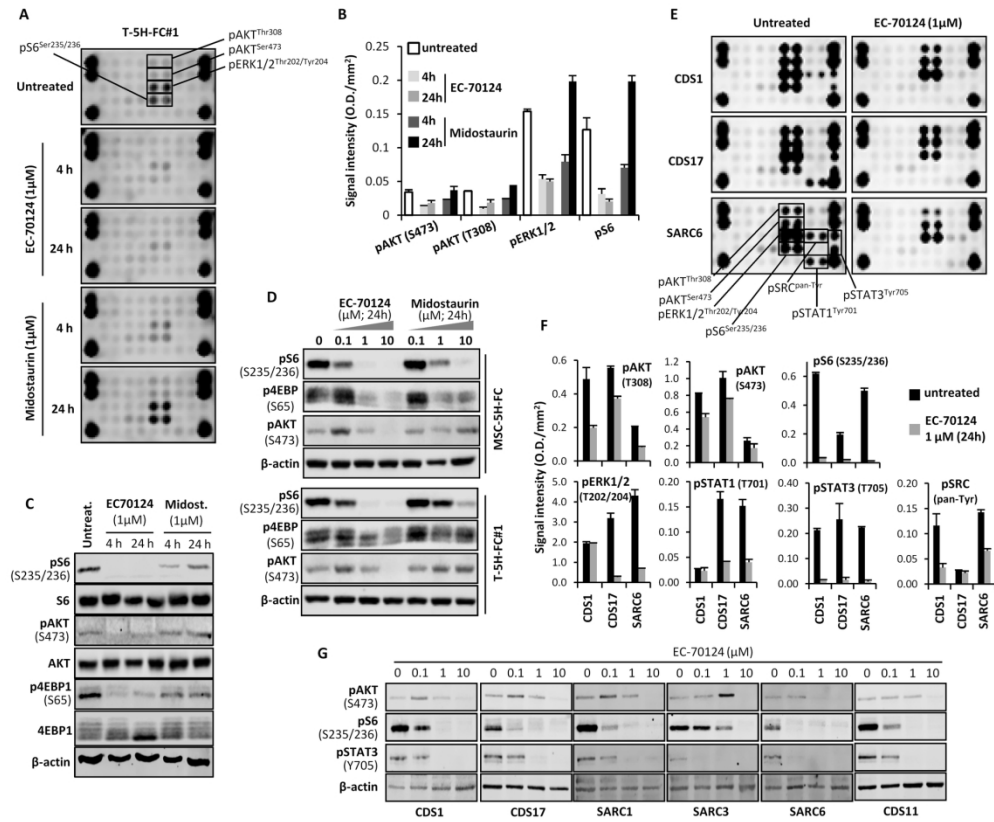
Estupiñan et al. Figure 1



Antiproliferative effects of EC-70124 and midostaurin in sarcoma

399x330mm (300 x 300 DPI)

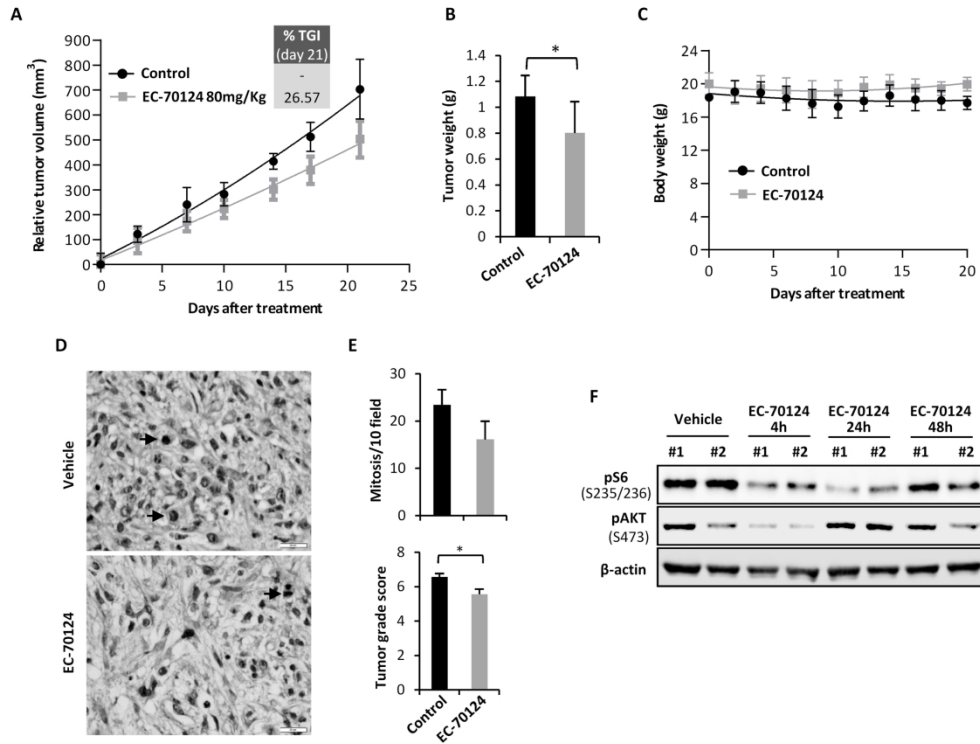
Estupiñan et al. Figure 2



Kinase inhibitory profile of EC-70124 and midostaurin

172x149mm (300 x 300 DPI)

Estupiñan et al. Figure 3

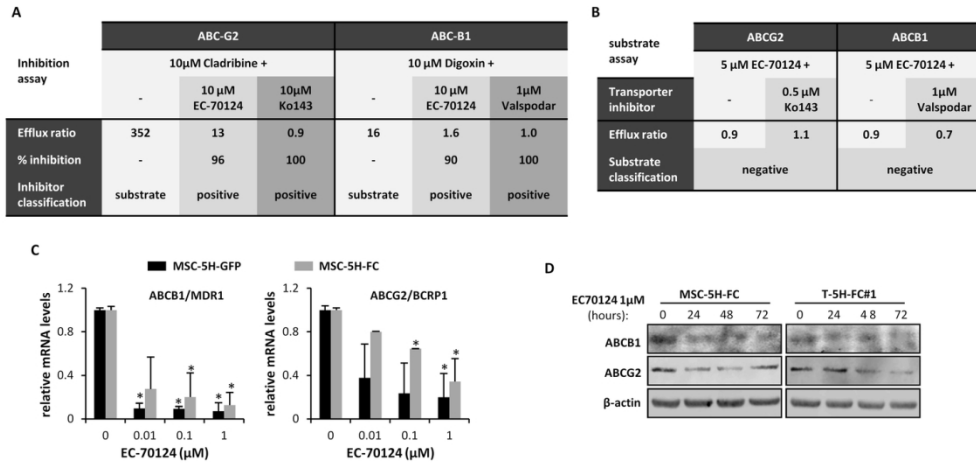


In vivo anti-tumor activity of EC-70124

206x169mm (300 x 300 DPI)



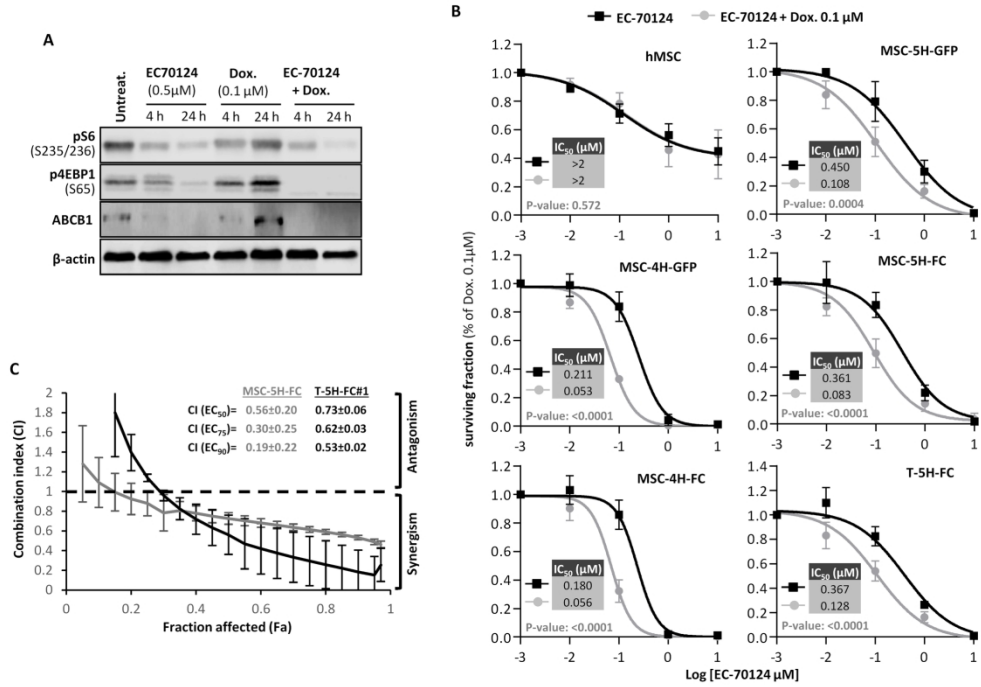
Estupiñan et al. Figure 4



Effect of EC-70124 on ABC transporters expression and activity

131x68mm (300 x 300 DPI)

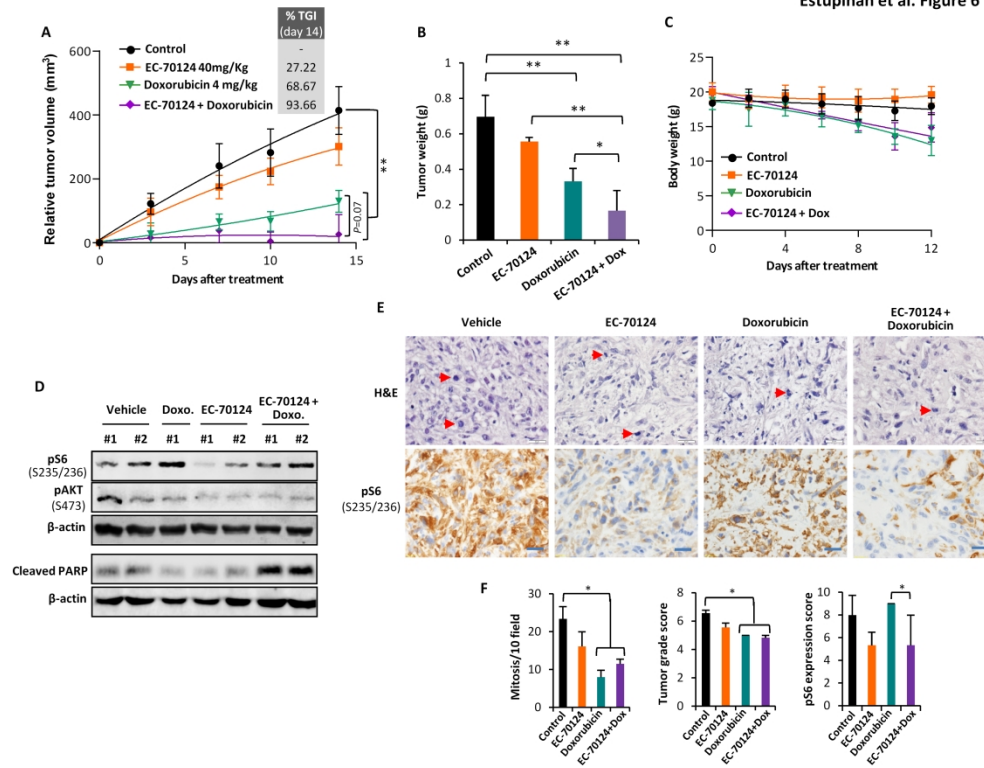
Estupiñan et al. Figure 5



EC-70124 and doxorubicin shows synergistic cytotoxic effect

193x150mm (300 x 300 DPI)

Estupiñan et al. Figure 6



In vivo effect of EC-70124 and doxorubicin combination

399x316mm (300 x 300 DPI)